






## Adsorption and porosity study of *Acacia catechu* seed derived activated carbon

Pawan Kumar Mishra<sup>1\*</sup>, Anant Ram<sup>2</sup>, Netra Prasad Subedi<sup>3</sup>, Dharendra Jha<sup>4</sup>, Madhab Gautam<sup>5</sup>

- 1 Department of Chemistry, R.R Multiple Campus, Janakpurdham, Tribhuvan University, Nepal.  
\*Corresponding Author ✉ [mishrapawanaz@gmail.com](mailto:mishrapawanaz@gmail.com)  [orcid.org/0009-0008-9568-6346](https://orcid.org/0009-0008-9568-6346)
- 2 Department of Chemistry, Lucknow University-226007 U.P, India.  
✉ [anant.ramchem@gmail.com](mailto:anant.ramchem@gmail.com)  [orcid.org/0009-0002-4481-6362](https://orcid.org/0009-0002-4481-6362)
- 3 Department of Chemistry, Central Campus of Technology, Dharan, Tribhuvan University, Nepal.  
✉ [netrasubedi007@gmail.com](mailto:netrasubedi007@gmail.com)  [orcid.org/0009-0001-6866-137X](https://orcid.org/0009-0001-6866-137X)
- 4 Department of Physics, R. R. Multiple Campus, Janakpurdham, Tribhuvan University, Nepal.  
✉ [dhiru2074@gmail.com](mailto:dhiru2074@gmail.com)  [orcid.org/0009-0003-1284-071X](https://orcid.org/0009-0003-1284-071X)
- 5 Department of Chemistry, Tribhuvan Multiple Campus, Palapa, Tribhuvan University, Nepal.  
✉ [madhab.gautam@tmc.tu.edu.np](mailto:madhab.gautam@tmc.tu.edu.np)  [orcid.org/0009-0007-4924-4275](https://orcid.org/0009-0007-4924-4275)

### ABSTRACT

Nowadays several biomasses based adsorbent materials are in practice. The activated carbon (AcC) shows efficient adsorption capacity. The pore size and surface morphology is essential for the best AcC that depends on the selection of activating agents. The aim of this study is to employ potassium Hydroxide (KOH) as a chemical activating agent for synthesizing AcC using *Acacia catechu* seeds through a carbonization process. Fourier-transform infrared spectroscopy (FTIR) was used to identify the functional groups present in carbonaceous materials while the X-ray diffraction (XRD) analysis was done for studying the crystalline nature of synthesized AcC. The surface morphology was studied with the help of image obtained from Field-Emission Electron Spectroscopy (FESEM). The iodine number (IN) and methylene blue number (MBN) for the sample activated with KOH (SACK-4) have been found to be 711.42 mg/g and 186.34 mg/g respectively which are much higher values in comparison to the corresponding numbers of non-activated sample (SACK-0), suggesting better adsorption performance of SACK-4. Furthermore, remarkable porosity has been achieved with SACK-4 that make it as a prominent candidate for different industrial and technical applications.

**Keywords:** *Acacia catechu* seed, Activated carbon, Iodine Number, Methylene Blue Number

### 1.0 Introduction

AcCs show remarkable performances when it is utilized as adsorbent systems so its potential applications have global demands in different disciplines (Chia *et al.*, 2022). The pivotal adsorptive characteristics of these materials is due to their micro-porous structure with the highly porous morphology (Daniel *et al.*, 2023). The porous morphology of AcCs is instrumental in determining their adsorptive efficacy and overall performance (El-Azazy *et al.*, 2021). Typically, these constituents are synthesized from precursors that possess a high C-content. The intrinsic behaviour of AcC is strongly influenced by the choice of precursor, the carbonization temperature, the activating agent, and the synthesis methodology (Gupta *et al.*, 2009). Thermal parameters govern structural transformations, pore development, and surface area characteristics, while techniques of preparation determine the chemical makeup, the presence of functional group, and overall capacity for adsorption (Hoan *et al.*, 2024). High-temperature carbonization plays a pivotal role in producing porous AcC, as higher temperatures promote the volatilization of organic compounds from the carbon matrix, so the formation of a porous structure gets enhanced (Imran & Rani, 2016).

AcC derived from numerous sources, including agricultural waste and renewable biomass, proves to be both economically advantageous and environmentally sustainable, ultimately contributing to a diminished dependence on bio-based fossil fuels (Jafari & Botte, 2023). The feasibility of synthesizing high-quality AcC, alongside accessibility and cost-effectiveness of raw materials, and the storing longevity of the materials, constitute prerequisite conditions for the selection of an optimal precursor material (Peh *et al.*, 2021). Chemical activation method is the best method to prepare highly porous AcCs at lower temperatures than other physical activation method (Li *et al.*, 2021). Biomass-derived AcCs can be prepared from various plants, and seeds derived from *Acacia catechu* is one of the promising and valuable source (Panagopoulou *et al.*, 2018). The reason behind this is the presence of lignocellulosic contents consisting of lignin, cellulose, hemicellulose etc. that makes it fit for carbonization as well as activation processes (Qin *et al.*, 2024). These lignocellulosic constituents make carbonaceous materials with high porosity which has sufficient adsorption performances and energy storage capability (Satpudke *et al.*, 2019).

Very few investigations were found for the effects of activating agents to adsorption performance and porosity of *Acacia catechu* seed derived AcC. Therefore, we tried to investigate effects of porosity and absorptivity of synthesized *Acacia catechu* derived AcCs in this present paper utilizing IN and MB adsorption tests. The primary goal was to examine the intrinsic biomass characteristics of seeds derived from *Acacia catechu* that contribute to their remarkable surface adsorption capabilities. Notably, the AcC produced with KOH at a constant temperature exhibited exceptionally high iodine and methylene blue adsorption capacities, underscoring its potential for diverse applications.

## **2.0 Experimental**

### **2.1 Collection and Pre-carbonization of Precursor material**

The seeds of *Acacia catechu* were procured in June 2021 from the Garambesi area located in Rainas-7, within the Lumjung region of Nepal. The harvested seeds stones underwent a shade dry for three months. Subsequently, the desiccated material was pulverized using a Herbal Disintegrator (FW 177) to obtain fine powdered form at Amrit Campus. Thus, prepared fine powder was pre-carbonized. Specifically, 50 g of an aliquot of the previously milled seed derived material was then followed by pyrolysis in the muffle furnace at 250 °C temperature for 3 hours. Thus, obtained pre-carbonized materials obtained from *Acacia catechu* seeds has been designated as SACK-0.

### **2.2 Activation Procedures**

Initially, 10 grams of pre-carbonized powder derived from *Acacia catechu* seeds and an equimolar KOH was thoroughly mixed for activation procedures. This mixture was converted into a fine paste with an agate mortar and pestle for 2 hours to achieve homogeneity. The prepared paste was then moved in a ceramic boat and allowed to stabilize at normal temperature for one day and night. Subsequently, the material obtained was then thermally activated at 400 °C under N<sub>2</sub> atmosphere. The resulting AcC was neutralized with 1M HCl and repeatedly washed with distilled water to remove residual impurities and made pH neutral. The product should be completely free from moisture and therefore, it was dried in hot-air oven around 80°C for 8 hours before vacuum drying for 6 hours. Finally, thus prepared dried material was made powder with mortar (agate), producing AcC fit for further characterization (Kumar *et al.*, 2018.). The synthesized sample was designated as SACK-4.

### 2.3 Determination of IN

The iodine number (IN) is utilized for determining microporosity of the AcC samples. For this analysis, 1 g of both (SACK-0 and SACK-4) samples were placed in separate conical flasks with 5 mL of 5% HCl. The suspensions were thoroughly agitated to ensure complete soaking, followed by boiling and subsequent cooling to normal temperature. Thereafter, 10 mL decinormal iodine solution was added to the flask, and the mixtures were shaken at the speed of 200 rpm for 10 minutes. After settling, the solutions were filtered using standard filter paper. The filtrate was titrated with 0.1 N sodium thiosulphate solution ( $\text{Na}_2\text{S}_2\text{O}_3$ ) (Miljanić *et al.*, 2007). A fresh starch as indicator was introduced so that a dark blue solution turned into straw yellow coloration and finally, became colorless. The IN-value was obtained using the following formula:

$$\text{IN} = \frac{\text{Amount of I}_2 \text{ in mg adsorbed by AC}}{\text{Wt. of AC taken in gram}} = \frac{\{(126.93N_I V_I) - [(V_I + V_{\text{HCl}})/V_F] \times (126.93N_{\text{Na}_2\text{S}_2\text{O}_3}) \times V_{\text{Na}_2\text{S}_2\text{O}_3}\}}{M_c} \quad (1)$$

Here,  $N_I$  = strength of iodine solution used (N),  $V_I$  = volume of iodine solution,  $V_{\text{HCl}}$  = volume of 5% HCl added,  $V_F$  = volume of filtrate used in titration,  $N_{\text{Na}_2\text{S}_2\text{O}_3}$  = strength of sodium thiosulfate solution,  $V_{\text{Na}_2\text{S}_2\text{O}_3}$  = volume of consumed sodium thiosulfate solution, &  $M_c$  = quantity of AcC.

### 2.4 Determination of MBN

For assessment of adsorbing capacity of prepared AcC, the MB adsorption method with batch experiments is utilized in this study. In this procedure, 0.1 g of both samples (SACK-0 and SACK-4) were mixed with 75 mL of 100 ppm MB solution. The suspensions were agitated on a shaker with the speed of 200 rpm for 4.5 hours at 25 °C, followed by a one-day equilibration period (Tadesse *et al.*, 2023). Subsequently, the mixtures were filtered using Whatman No. 42 filter paper, and the lingering MB concentration as the filtrate was determined with a spectrophotometer (Labtronics, LT-2802). The quantity of MB adsorbed (mg/g) in a given time (t), was calculated using the formula:

$$\text{MBN} = \frac{(C_0 - C_e)V}{W}, \quad (2)$$

where,  $C_0$  and  $C_e$  are initial and balance MB solution concentrations (mg/L or ppm), respectively,  $W$  signifies the amount of the adsorbent (g), and  $V$  is the volume of the solution (L).

## 3.0 Results and Discussions

### 3.1 Functional group analysis

FTIR-spectroscopy gives the indication of AcC material. The surface and adsorption performances of AcCs derived from seeds are suggestively influenced by the existence of functional groups with heteroatoms like oxygen atom (Danish *et al.*, 2018). The FTIR spectra for seed-derived AcC samples are shown in Fig.1.

The FTIR spectra of all analyzed samples revealed notable similarities, regardless of the activating agents employed in their preparation. Distinct absorption bands were observed in the wavenumber region of 700–1700  $\text{cm}^{-1}$  (Bai *et al.*, 2019). The peak near 1700  $\text{cm}^{-1}$  refers to the stretching vibrations of carbonyl bonds, representing the presence of ketonic or aldehyde groups in the AcC derived from *Acacia catechu* seeds. Similarly, the prominent peak near 1461  $\text{cm}^{-1}$  is attributed to C–C stretching vibrations, while the peak at approximately 1600  $\text{cm}^{-1}$  indicates the highly conjugated C=O stretching linked with benzene ring systems (Kumar *et al.*, 2022). The absorption bands between 1100 and 1200  $\text{cm}^{-1}$  are characteristic of C–O

stretching, and a weak band somewhat above  $3000\text{ cm}^{-1}$  corresponds to unsaturated alkene C=C stretching at around band somewhat above  $3000\text{ cm}^{-1}$  corresponds to unsaturated alkene C=C stretching at around  $1620\text{ cm}^{-1}$ . In addition, the peaks in the  $860\text{--}600\text{ cm}^{-1}$  range indicate aromatic C–H bending (Ali *et al.*, 2020) whereas a weak peak near  $3740\text{ cm}^{-1}$  is linked to O–H stretching of phenolic or alcoholic groups (Mishra *et al.*, 2024). Overall, the FTIR spectra confirm the incidence of oxygen-containing surface functional groups suggesting lactones, carboxyl, carbonyl, and hydroxyl groups across all AcC samples (González-García, 2018).

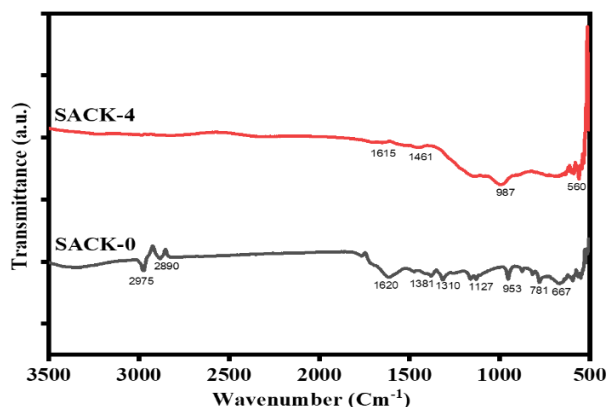


**Figure 1:** FTIR spectra of prepared SACK-0 and SACK-4 samples.

### 3.2. X-ray diffraction (XRD) characterization

The structural purity condition as well as crystalline behaviour of KOH-AcC were examined using XRD analysis. The diffraction patterns ascertained the phase purity of AcC samples, displaying broad peaks characteristic of carbonaceous materials, with no proof of residual activating agents, thereby supporting the successful fusion of pure AcC. XRD patterns of SACK-0 and SACK-4 at the  $2\theta$  range of  $10^\circ\text{--}90^\circ$  are shown in Fig.2. Both SACK-0 and SACK-4 samples showed broad yet distinct diffraction peaks, including a prominent peak at  $2\theta \approx 25.51^\circ$  with a d-spacing of approximately 0.33 nm and indexed to the (002) plane, indicative of graphitic carbon structures. Furthermore, a secondary peak at  $2\theta \approx 43.69^\circ$  provides additional confirmation of the carbonaceous nature of the materials (Bestani *et al.*, 2008).

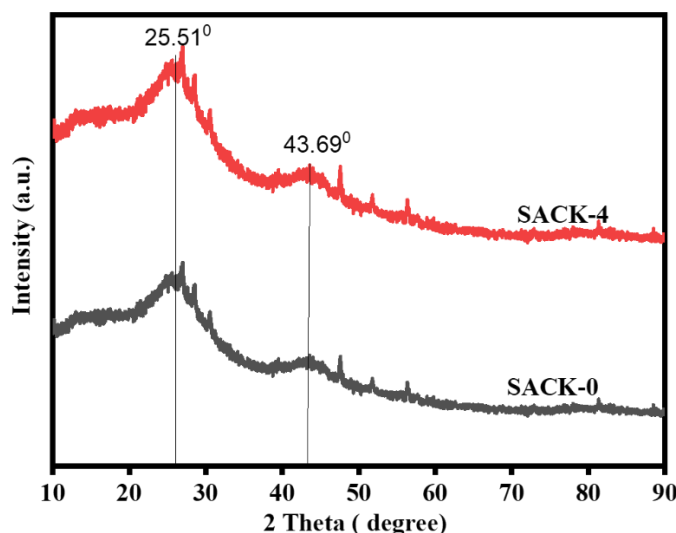


**Figure 2:** XRD of Pre-carbonized sample (SACK-0) and Activated sample (SACK-4).

### 3.3 Iodine and methylene blue number

The AcC recital is commonly evaluated using iodine and MB adsorption techniques, as these methods give crucial insights into pore size distribution and structural characteristics. Iodine adsorption reflects the capacity to capture small molecules due to the relatively minor molecular size of iodine (Nunes & Guerreiro, 2011), whereas the methylene blue number (MBN) is primarily used to quantify mesoporous structures (Shrestha *et al.*, 2019).

The IN of the samples is illustrated in Fig. 3(a). The KOH-AcC prepared at 400 °C (SACK-4) exhibited the highest iodine number of 711.42 mg/g, compared to the non-AcC prepared at 250 °C, which displayed a significantly lower value of 219.09 mg/g. These findings indicate that microporous structure development in the synthesized AcC is governed not only by the activation temperature but also by the activating agent and its specific interactions with the precursor.

Furthermore, changes in the concentration of MB before and after adsorption by synthesized AcC was monitored with MB number. Absorbance was measured with a spectrophotometer, and the mesopore content was estimated based on these values (Shrestha *et al.*, 2019; Xie *et al.*, 2013). The maximum absorbance wavelength of the methylene blue solution was recorded at 665 nm. As shown in Fig. 3(b), the SACK-4 sample achieved a markedly higher adsorption capacity (186.34 mg/g) than SACK-0 (88.7 mg/g), confirming a greater mesopore content.

The enhancement of microporosity and mesoporosity in KOH-AcC is attributed to the combined effects of elevated temperatures and chemical activation. High temperatures promote the removal of volatile components from the precursor and expand pore structures, while KOH actively reacts with the carbon matrix, producing gaseous byproducts such as CO and CO<sub>2</sub> (Yu *et al.*, 2019). This chemical reactivity facilitates deeper penetration of the activating agent, thereby enhancing gasification reactions and promoting efficient pore formation (Abdul Khalil *et al.*, 2013). Reactive intermediates such as potassium carbonate and metallic potassium, generated during activation, catalyze pore development (Zhang *et al.*, 2020; Sundriyal *et al.*, 2021). Additionally, the small ionic radius and high mobility of potassium ions contribute to uniform pore distribution and structural expansion. Activation at the optimal temperature of 400 °C further enhances gas evolution and pore generation (Ghobashy & Abdeen, 2016). Collectively, these mechanisms account for the increased surface area and the simultaneous enhancement of microporosity and mesoporosity in KOH-AcC (Mishra *et al.*, 2025).

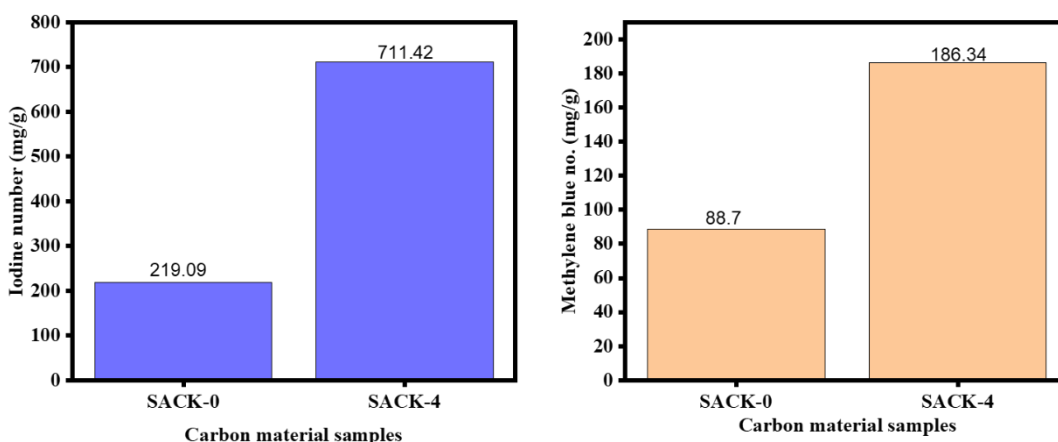


**Figure 3:** Bar graph demonstrating (a) iodine number and (b) methylene blue number of samples (SACK-0 and SACK-4).

### 3.4 Field Emission Scanning Electron Microscopy (FESEM)

The surface morphology related structural information of the carbon materials was scrutinized by FESEM. Figure 4 (a, b) depicts the FESEM surface image of SACK-0 and SACK-4 at magnification X5000.

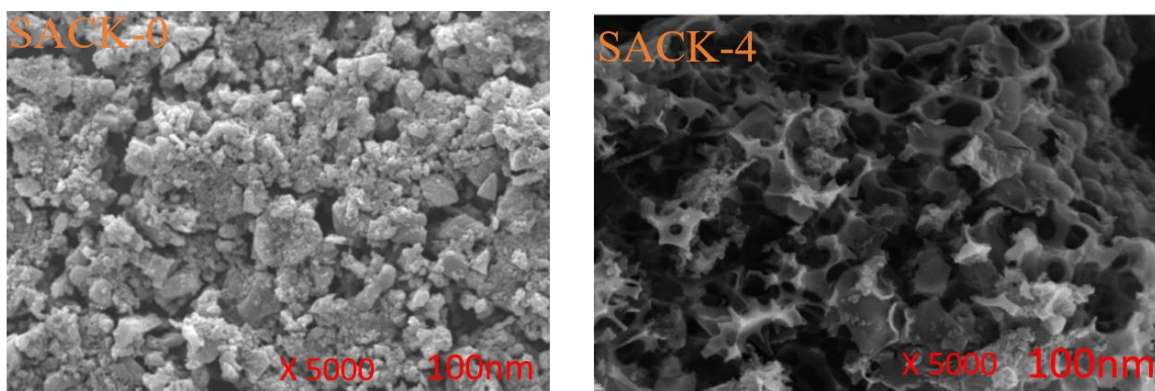


**Figure 4:** Morphological study: FESEM image of (a) SACK-0 and (b) SACK-4.

These microstructural images highlight the pronounced influence of activating agents on the surface morphology and porosity of carbon samples. As shown in Fig. 4(a), the pre-carbonized char exhibits a relatively smooth surface with negligible porosity, indicating an almost non-porous nature. In contrast, the KOH-AcC, depicted in Figure 4(b), displays a highly porous and interconnected structure, reflecting a greater degree of activation and pore formation. Nevertheless, the pore distribution is not completely uniform, suggesting that activation occurs in a localized manner. The clear differences between the pore structures of inactivated and KOH-AcC underscore the distinct mechanisms involved (Mishra *et al.*, 2025). Specifically, KOH activation proceeds through surface etching, followed by gasification of lignocellulosic components released from the carbon matrix, ultimately generating a porous architecture (Bhungthong *et al.*, 2017).

### 4.0 Conclusion

Biomass or *Acacia catechu* seed-derived activated carbon (AcC) adsorbents have gained increasing attention in these days due to their eco-friendly and non-toxic characteristics. In this investigation, the potential of using *Acacia catechu* seed materials for the preparation of nanoporous AcC was systematically investigated. The synthesis process employed a chemical activation route in which potassium hydroxide (KOH) served as the activating agent at 400 °C. The physicochemical characteristics of the synthesized AcC materials were examined through FTIR, XRD, FESEM, IN, and MBN analyses. The outcomes demonstrated that KOH activation plays a decisive role in generating AcC (SACK-4) with a highly developed porous network. This effect can be attributed to KOH's strong reactivity, efficient ion transport, and catalytic gasification properties. The superior porosity was further validated by the elevated iodine and methylene blue adsorption values, recorded as 711.42 mg/g and 186.34 mg/g, respectively. These findings were consistent with FESEM images that revealed a well-structured surface morphology. When compared to non-activated carbon, the KOH-activated sample exhibited markedly enhanced adsorption performance. Taken together, the lignocellulosic content of *Acacia catechu* seeds and the efficiency of KOH activation establish this approach as a cost-effective and scalable strategy for the development of high-performance adsorbents. The major applications of this adsorbent material obtained from *Acacia catechu* seed derived activated



carbon are water purification as well as EDLC (electric double layer capacitor) negative electrode materials in energy storage device for supercapacitor applications.

### Conflict of interests

The authors declare that neither financial interests nor personal relationships had any impact on the work described in this paper.

### Acknowledgements

Authors acknowledge the partial financial funding provided by the University Grant Commission (UGC) and are thankful to Amrit campus for laboratory support.

### References

- Abdul Khalil, H.P.S., Jawaid, M., Firoozian, P., Rashid, U., Islam, A., & Akil, H.M. (2013). Activated carbon from various agricultural wastes by chemical activation with KOH: Preparation and characterization. *Journal of Biobased Materials and Bioenergy*, 7(6), 708–714. <https://doi.org/10.1166/jbmb.2013.1379>
- Ali, R., Aslam, Z., Shawabkeh, R.A., Asghar, A., & Hussein, I.A. (2020). BET, FTIR, and RAMAN characterizations of activated carbon from waste oil fly ash. *Turkish Journal of Chemistry*, 44(2), 279–295. <https://doi.org/10.3906/KIM-1909-20>
- Bai, P., Wei, S., Lou, X., & Xu, L. (2019). An ultrasound-assisted approach to bio-derived nanoporous carbons: Disclosing a linear relationship between effective micropores and capacitance. *RSC Advances*, 9(54), 31447–31459. <https://doi.org/10.1039/c9ra06501f>
- Bestani, B., Benderdouche, N., Benstaali, B., Belhakem, M., & Addou, A. (2008). Methylene blue and iodine adsorption onto an activated desert plant. *Bioresource Technology*, 99(17), 8441–8444. <https://doi.org/10.1016/j.biortech.2008.02.053>
- Bhungthong, S., Aussawasathien, D., Hrimchum, K., & Sriphalang, S.N. (2017). Effects of processing parameters on properties of activated carbon from palm shell: Sodium hydroxide impregnation. *Chiang Mai Journal of Science*, 44(2), 544–556.
- Chia, C.H., Zakaria, S., Sajab, M.S., & Saad, M.J. (2022). Activated Carbon Produced from Rice Husk by NaOH and KOH Activation and its Adsorption in Methylene Blue. *Advances in Agricultural and Food Research Journal*, 3(2), 1–13. <https://doi.org/10.36877/aafj.a0000297>
- Daniel, L.S., Rahman, A., Hamushembe, M.N., Kapolo, P., Uahengo, V., & Jonnalagadda, S.B. (2023). The production of activated carbon from *Acacia erioloba* seedpods via phosphoric acid activation method for the removal of methylene blue from water. *Bioresource Technology Reports*, 23, 101568. <https://doi.org/10.1016/j.biteb.2023.101568>
- Danish, M., Ahmad, T., Majeed, S., Ahmad, M., Ziyang, L., Pin, Z., & Shakeel Iqbal, S.M. (2018). Use of banana trunk waste as activated carbon in scavenging methylene blue dye: Kinetic, thermodynamic, and isotherm studies. *Bioresource Technology Reports*, 3, 127–137. <https://doi.org/10.1016/j.biteb.2018.07.007>
- El-Azazy, M., El-Shafie, A.S., & Yousef, B.A.S. (2021). Green tea waste as an efficient adsorbent for methylene blue: Structuring of a novel adsorbent using full factorial design. *Molecules*, 26(20). <https://doi.org/10.3390/molecules26206138>
- Ghobashy, M.M., & Abdeen, Z.I. (2016). Radiation Crosslinking of Polyurethanes: Characterization by FTIR, TGA, SEM, XRD, and Raman Spectroscopy. *Journal of*

## *Adsorption and porosity study of Acacia Catechu seed derived activated carbon*

*Polymers*, 2016, 1–9. <https://doi.org/10.1155/2016/9802514>

- González-García, P. (2018). Activated carbon from lignocellulosic precursors: A review of the synthesis methods, characterization techniques and applications. *Renewable and Sustainable Energy Reviews*, 82, 1393–1414. <https://doi.org/10.1016/j.rser.2017.04.117>
- Gupta, V.K., Carrott, P.J.M., Ribeiro Carrott, M.M.L., & Suhas. (2009). Low-Cost adsorbents: Growing approach to wastewater treatment review. *Critical Reviews in Environmental Science and Technology*, 39(10), 783–842. <https://doi.org/10.1080/10643380801977610>
- Hoan, L.T., Chinh, T.V., Anh, L.Q., Lam, N.P., Hien, H.P., Duong, L.D., Nga, T.T., & Ha, N.M. (2024). Synthesis of activated carbon from pet plastic waste by H<sub>3</sub>PO<sub>4</sub> activator for environmental treatment application. *HaUI Journal of Science and Technology*, 60(11), 199–207.
- Imran Din, M., & Rani, A. (2016). Recent advances in the synthesis and stabilization of nickel and nickel oxide nanoparticles: a green adeptness. *International journal of analytical chemistry*, 2016(1), 3512145.
- Jafari, M., & Botte, G.G. (2023). Sustainable Green Route for Activated Carbon Synthesis from Biomass Waste for High-Performance Supercapacitors. *ACS Omega*, 9(11), 13134–13147. <https://doi.org/10.1021/acsomega.3c09438>
- Peh, S., Wang, Y., & Zhao, D. (2019). Scalable and sustainable synthesis of advanced porous materials. *ACS Sustainable Chemistry & Engineering*, 7(4). <https://doi.org/10.1021/acssuschemeng.8b05463>
- Kumar, D., Thakur, C.L., & Bhardwaj, D.R. (2022). Biodiversity conservation and carbon storage of *Acacia catechu* wild. Dominated northern tropical dry deciduous forest ecosystems in North-Western Himalaya: Implications of different forest management regimes. *Frontiers in Environmental Science*. 10, 1–16, 981608. <https://doi.org/10.3389/fenvs.2022.981608>
- Kumaresen, T.K., Sundari, G.S., Kumar, E.S., Ashwini, A., & Raghu, S. (2018). Synthesis of Nanoporous Carbon with New Activating Agent for high- performance Supercapacitor. *Materials Letters*. 218, 181–184. <https://doi.org/10.1016/j.matlet.2018.02.017>
- Li, S., Zhu, Y., Wang, Y., & Liu, J. (2021). The chemical and alignment structural properties of coal: Insights from Raman, Solid-State <sup>13</sup>C NMR, XRD, and HRTEM Techniques. *ACS Omega*, 6(17), 11266–11279. <https://doi.org/10.1021/acsomega.1c00111>
- Miljanić, S., Frkanec, L., Biljan, T., Meić, Z., & Žini, C.M. (2007). Recent Advances in linear and nonlinear Raman spectroscopy. *Journal of Raman Spectroscopy*, 38, 1538–1553. <https://doi.org/10.1002/jrs>
- Mishra, P.K., Aryal, S., Oli, H.B., Shrestha, T., Jha, D., Shrestha, R.L., & Bhattarai, D.P. (2025). Porosity Analysis of *Acacia catechu* Seed-derived Carbon Materials Activated with Sodium Hydroxide and Potassium Hydroxide: Insights from Methylene Blue and Iodine Number Methods. *Journal of Nepal Chemical Society*, 45(1), 57–65. <https://doi.org/10.3126/jncs.v45i1.74387>
- Mishra, P.K., Aryal, S., Oli, H.B., Shrestha, T., Md.al-Mamun, Shrestha, R.L., & Bhattarai, D.P. (2024). Enhanced energy storage: Electrochemical performance of ZnCl<sub>2</sub>-activated carbon derived from *Acacia catechu* Bark. *Mongolian Journal of Chemistry*, 25(52), 26–34. <https://doi.org/10.5564/mjc.v25i52.3501>
- Nunes, C.A., & Guerreiro, M.C. (2011). Estimation of surface area and pore volume of



- activated carbons by methylene blue and iodine numbers. *Quimica Nova*, 34(3), 472–476. <https://doi.org/10.1590/S0100-40422011000300020>
- Panagopoulou, A., Lampakis, D., Christophilos, D., Beltsios, K., & Ganetsos, T. (2018). Technological examination of Iznik ceramics by SEM-EDX, Raman, XRD, PLM: A case study. *Scientific Culture*, 4(3), 27–33. <https://doi.org/10.5281/zenodo.1409802>
- Qin, Q., Wang, J., Tang, Z., Jiang, Y., & Wang, L. (2024). Mesoporous activated carbon for supercapacitors derived from coconut fiber by combining H<sub>3</sub>PO<sub>4</sub>-assisted hydrothermal pretreatment with KOH activation. *Industrial Crops and Products*, 208, 117878. <https://doi.org/10.1016/j.indcrop.2023.117878>
- Satpudke, S., Pansare, T., & Khandekar, S. (2019). Review on Arjuna (*Terminalia Arjuna* Roxb.) With Special Reference to Prameha (Diabetes). *International Journal of Herbal Medicine*, 8(6), 1–5. <https://www.florajournal.com/archives/2020/vol8issue1/PartA/7-4-57-649.pdf>
- Shrestha, L.K., Thapa, M., Shrestha, R.G., Maji, S., Pradhananga, R.R., & Ariga, K. (2019). Rice Husk-Derived High Surface Area Nanoporous Carbon Materials with Excellent Iodine and Methylene Blue Adsorption Properties. *C Journal of Carbon Research*, 5(1), 10. <https://doi.org/10.3390/c5010010>
- Sundriyal, S., Shrivastav, V., Duc, H., Mishra, S., Deep, A., & Dubal, D.P. (2021). Resources, Conservation & Recycling Advances in bio-waste derived activated carbon for supercapacitors: trends, challenges and prospective. *Resources, Conservations and Recycling*, 169, 105588. <https://doi.org/10.1016/j.resconrec.2021.105548>
- Tadesse, M.G., Kasaw, E., & Lübben, J.F. (2023). Valorization of banana peel using carbonization: potential use in the sustainable manufacturing of flexible super capacitors. *Micromachines*, 14(2), 330. <https://doi.org/10.3390/mi14020330>
- Xie, L.J., Wu, J.F., Chen, C.M., Zhang, C.M., Wan, L., Wang, J.L., Kong, Q.Q., Lv, C.X., Li, K.X., & Sun, G.H. (2013). A novel asymmetric supercapacitor with an activated carbon cathode and a reduced graphene oxide-cobalt oxide nanocomposite anode. *Journal of Power Sources*, 242, 148–156. <https://doi.org/10.1016/j.jpowsour.2013.05.081>
- Yu, D., Ma, Y., Chen, M., & Dong, X. (2019). KOH activation of wax gourd-derived carbon materials with high porosity and heteroatom content for aqueous or all-solid-state supercapacitors. *Journal of Colloid and Interface Science*, 537, 569–578. <https://doi.org/10.1016/j.jcis.2018.11.070>
- Zhang, H., Han, X., Gan, R., Guo, Z., Ni, Y., & Zhang, L. (2020). A facile biotemplate-assisted synthesis of mesoporous V<sub>2</sub>O<sub>5</sub> microtubules for high performance asymmetric supercapacitors. *Applied Surface Science*, 511, 145527. <https://doi.org/10.1016/j.apsusc.2020.145527>